00-013

Modeling Biofilm Antimicrobial Resistance

Michael G. Dodds,* Katherine J. Grobe, Philip S. Stewart

Center for Biofilm Engineering, and Department of Chemical Engineering, Montana State University, Bozeman, Montana 59717; telephone: (406) 994-2890; fax: (406) 994-6098; e-mail: phil_s@erc.montana.edu

Received 1 July 1999; accepted 27 November 1999

Abstract: A computer model capable of integrating mechanisms of biofilm resistance to disinfection by antimicrobial agents was developed. Resistance mechanisms considered included retarded penetration due to a stoichiometric reaction between the antimicrobial agent and biomass, incomplete penetration due to a catalytic reaction between the antimicrobial agent and the biomass, and the existence of a fraction of the cells in a resistant phenotypic state. Mathematical models of these processes were derived and solved in the computer simulation package MATLAB. Four sets of fitted experimental data on the disinfection of *Pseudomonas aeruginosa* biofilms were fit to each of the three models. No one model fit all of the data sets adequately. Killing of a 2-day old biofilm by tobramycin was best described by the physiological limitation model. Killing by hypochlorite was best described by the stoichiometric transport model. Killing by hydrogen peroxide was best simulated by the catalytic transport model. These results suggest that multiple mechanisms of biofilm reduced susceptibility are manifested even in biofilms of the same species and that the particular resistance mechanism depends on the biofilm age, antimicrobial agent, and biofilm thickness. The models presented in this article may be useful for diagnosing mechanisms of biofilm resistance from experimental data. © 2000 John Wiley & Sons, Inc. *Biotechnol Bioeng* 68: 456–465, 2000.

Keywords: biofilm; antimicrobial; disinfection; reaction-diffusion; model; resistance

INTRODUCTION

Microorganisms growing in the form of a surface-attached biofilm are ubiquitous in aquatic systems. When biofilms accumulate in engineered systems, such as oilfield pipelines or food processing equipment, they contribute to problems including fouling, corrosion, and product contamination (Characklis and Marshall, 1990). In medicine, biofilms are responsible for numerous difficult to manage infections (Costerton et al., 1999). Antimicrobial agents are widely used to control biofilm formation, but they are universally found to be less effective against biofilm cells than they are against cells of the same microbial strain grown in conventional suspension cultures (Costerton et al., 1987; Gilbert and Brown, 1993).

The mechanisms by which microorganisms in a biofilm evade killing by disinfectants, biocides, and antibiotics are of obvious practical interest and are just beginning to be discovered. It is now clear that there must be multiple resistance mechanisms. One of these is failure of the antimicrobial agent to penetrate the full depth of the biofilm. Although effective diffusion coefficients of solutes in biofilms are reduced somewhat from their values in water (Stewart, 1998), diffusioin in biofilms occurs relatively freely. The inherent mobility of antimicrobial agents within the biofilm is unlikely to be restricted enough to account for the profoundly reduced susceptibility of biofilm microorganisms. It is only when the antimicrobial agent is reactively neutralized in the surface layers of the biofilm faster than it duffuses into the biofilm interior that penetration limitation occurs. This mechanism, a twist on the reaction-diffusion interactions that have long been discussed in the chemical and biochemical engineering literature, has been demonstrated experimentally for reactive oxidants such as chlorine (de Beer et al., 1994; Chen et al., 1996; Xu et al., 1998), hydrogen peroxide (Liu et al., 1998), as well as other biocides (Stewart et al., 1998). In contrast, a number of experimental studies have demonstrated that certain antibiotics permeate biofilms readily (Nichols et al., 1989; Dunne et al., 1993; Darouiche et al., 1994; Suci et al., 1994; Shigeta et al., 1997; Vrany et al., 1997). The ability of these agents to penetrate depends on their not being prone to deactivation in the biofilm. Even when the antimicrobial agent is not particularly reactive or when the biofilm is very thin, biofilm microorganisms can display remarkable resistance to killing. Some other resistance mechanism must be at work because penetration limitation is not a tenable theory under these conditions.

The other major hypothesis to explain biofilm reduced susceptibility to antimicrobial agents requires that at least some fraction of the cells in a biofilm inhabit zones of nutrient depletion and adopt a slow-growing or starvation-like physiological state (Brown and Gilbert, 1988; Gilbert and Brown, 1995; Desai et al., 1998; Foley et al., 1999). Since slow-growing or starved cells are known to be less susceptible to many types of inimical challenges, biofilm

* *Present address:* Dept. of Bioengineering, University of Washington, Seattle, WA 98195-7962.

Correspondence to: P. S. Stewart

Contract grant sponsor: NSF and Montana State University
Contract grant number: BEC-8907039

recalcitrance could be explained. This mechanism is supported by experimental demonstrations of striking spatial heterogeneity in the physiological status of biofilm bacteria (Wentland et al., 1996; Huang et al., 1998; Xu et al., 1998) and by experimental results that are generally consistent with a correlation between biofilm growth rate and antibiotic susceptibility (Gilbert and Brown, 1995).

Mathematical modeling is a useful tool in the effort to elucidate biofilm reduced susceptibility because it allows hypotheses to be formulated and tested in quantitative terms. Several modeling studies of biofilm resistance have been reported (Stewart, 1994, 1996; Stewart and Raquepas, 1995; Dibdin et al., 1996; Stewart et al., 1996). Another potential benefit of modeling that has not been tapped to date is the ability to diagnose resistance mechanisms. The purpose of this study was to develop simplified models of biofilm antimicrobial resistance incorporating a physiological limitation and two transport limitation mechanisms of biofilm resistance. The face validity and potential applicability of the models were investigated by fitting several data sets of biofilm killing from the literature and our own laboratories.

THEORY

Three models of biofilm antimicrobial resistance were derived in this work. These models were based on the following conceptual scenarios. (1) Physiological limitation of biofilm susceptibility: The biofilm harbors cells in two states, one of which is relatively resistant to killing. Complete penetration of the antimicrobial agent is assumed in this case. (2) Transport limitation of a stoichiometrically reacting antimicrobial agent: The agent eventually fully penetrates, but it must deplete the fixed neutralizing capacity of the biofilm first. No physiological limitation is assumed in this case. (3) Transport limitation of a catalytically reacting antimicrobial agent: the extent of penetration is determined by the steady-state balance of reaction and diffusion. No physiological limitation is assumed in this case. Features of the three models are summarized in Table I.

The models share some assumptions. All of the models are based on a one-dimensional slab biofilm geometry and a uniform total cell density throughout the biofilm. The bulk fluid contains antimicrobial agent at a constant concentration. External mass transfer resistance is neglected. An impermeable substratum is assumed. No detachment occurs during the treatment period. The conceptual basis for the constituent models is explained in more detail below.

Table I. Summary of models (DOF denotes degrees of freedom).

Model	Symbol	DOF	Parameters
Physiological limitation	P	3	k_{dis}, ε_r, p
Stoichiometric transport	S	2	k_{dis}, t_{pen}
Catalytic transport	C	2	k_{dis}, ϕ

Physiological Limitation Model

The biofilm is assumed to contain cells in two phenotypic states: resistant and susceptible. These two populations are spatially segregated. The resistant population resides adjacent to the substratum and the susceptible population adjacent to the biofilm–bulk fluid interface (Fig. 1A). This hypothesized spatial distribution is based on the expected location of nutrient replete and limited zones and is consistent with recent experimental visualizations of physiological heterogeneity (Wentland et al., 1996; Huang et al., 1998; Xu et al., 1998). The susceptible population, whose fraction of the total population is denoted by ε_s on Fig. 1, has the same susceptibility as a planktonic cell to a chemical attack. The resistant cell fraction, denoted by ε_r on Fig. 1, enjoys a reduced susceptibility.

Because the antimicrobial agent is assumed to completely penetrate the biofilm in the physiological limitation model, the particular spatial distribution of sensitive and resistant cells is not important. A spatially segregated model is presented here because in subsequent work we have integrated the physiological limitation and transport models. In these combined models the spatial distribution of the cell types is obviously critical.

The derivation of the physiology model is rooted in a basic disinfection model which we generalize to allow for spatial variation with

$$\frac{dX}{dt} = -k_{dis}(z)\, C(z,t)\, X(t). \tag{1}$$

In this equation, X denotes the concentration of viable cells, C the concentration of antimicrobial agent, z position in the biofilm with $z = 0$ corresponding to the biofilm–bulk fluid interface, and t time. The disinfection rate coefficient depends on position in the biofilm. In the outer and susceptible portion of the biofilm, the disinfection rate coefficient is equal to the disinfection rate coefficient of a suspended planktonic culture, k_{dis}. In the deeper resistant zone of the biofilm, the disinfection rate coefficient is taken to be a fraction of the suspended culture disinfection rate coefficient. That fraction, denoted by p here, is smaller than 1.

Experimental data on biofilm disinfection are collected by scraping and resuspending the biofilm, then enumerating surviving cells. For comparison to experimental data, therefore, it is useful to calculate the "average survival fraction" of the biofilm as a whole. Integrating the general disinfection equation (1) across the extent of the biofilm yields the average survival fraction:

$$\int_0^1 \frac{X}{X_o}\, d\xi = \int_0^1 \exp(-k_{dis} C_b t_{dose})\, d\xi. \tag{2}$$

The disinfection rate coefficient is defined as:

$$k_{dis}(\xi) = \begin{cases} k_{dis} & \text{for } \varepsilon_s \geq \xi \geq 0, \\ p \cdot k_{dis} & \text{for } 1 \geq \xi > \varepsilon_s. \end{cases}$$

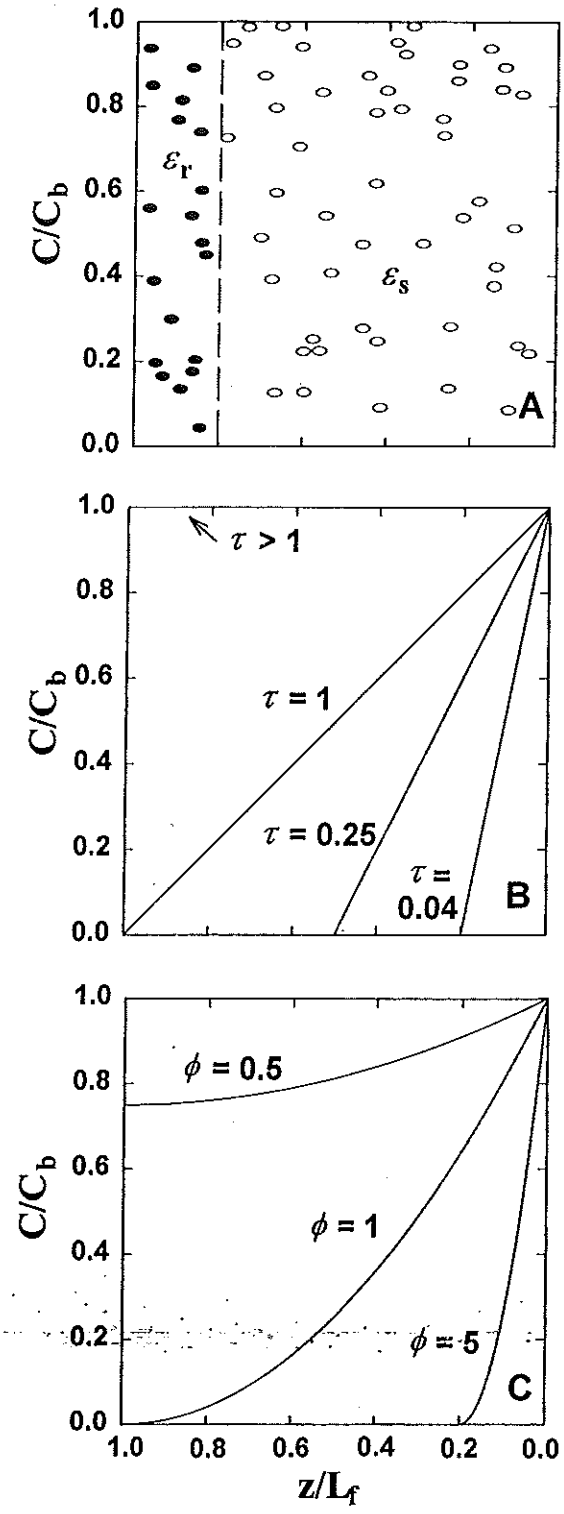

Figure 1. Conceptual basis of three models of biofilm antimicrobial resistance. The substratum is at the left and the bulk fluid is at the right in each panel. (A) Physiological limitation model. The biofilm exhibits physiological heterogeneity. Resistant cells (shaded black) reside adjacent to the substratum and susceptible cells (no shading) adjacent to the biofilm–bulk fluid interface. (B) Stoichiometric transport limitation model. Antimicrobial agent gradually penetrates the biofilm as the dimensionless time, τ, increases. (C) Catalytic transport limitaiton model. The curves correspond to concentration profiles of antimicrobial agent within the biofilm calculated according to a zero-order kinetic reaction-diffusion model, with the corresponding value of the Thiele modulus indicated. These concentration profiles are assumed to be established rapidly then to persist in time indefinitely.

Then, splitting the solutions to Eq. (2) into two parts yields:

$$\int_0^1 \frac{X}{X_o} \cdot d\xi = \int_0^{\varepsilon_s} \exp(-\psi)\, d\xi + \int_{\varepsilon_s}^1 \exp(-p\psi)\, d\xi, \quad (3)$$

where $\psi \equiv k_{dis} \cdot C_b \cdot t_{dose}$.

Of the models presented here, only the physiological limitation model has a closed form analytical solution available:

$$\int_0^1 \frac{X}{X_o}\, d\xi = (1 - \varepsilon_r) \exp(-\psi) + \varepsilon_r \exp(-p\psi). \quad (4)$$

Stoichiometric Transport Model

The biofilm is assumed to contain a finite, uniformly distributed amount of neutralizing capacity, which will be depleted stoichiometrically as the antimicrobial agent penetrates the biofilm. Reaction between the antimicrobial agent and neutalizing constituents of the biofilm is assumed to be independent of cell viability. This reaction is furthermore assumed to be relatively fast so that the reaction is confined to a very narrow zone in the biofilm. The anticipated movement of the reaction front through the biofilm is depicted schematically in Figure 1B and is qualitatively similar to experimentally measured data for chlorine penetration in an artificial biofilm system (Chen et al., 1996). Once the antimicrobial agent reaches the substratum there is little left to impede its progress and breakthrough or saturation occurs. In the model, the antimicrobial concentration is assumed to jump to the bulk fluid concentration throughout the biofilm at this time.

The mathematics of the stoichiometric transport model are derived by combining the basic disinfection model (1) with a linear concentration profile of C in z:

$$C(z,t) = \begin{cases} 0, & 0 \le t \le t_1, \\ C_b - C_b \cdot \dfrac{z}{a}, & t_1 \le t \le t_{pen}, \quad 0 \le z \le L_f, \\ C_b, & t_{pen} \le t \le \infty, \end{cases} \quad (5)$$

The boundary conditions are expressed in the form of t, while the equation is in z. A conversion of the equation to time dependence is required. The penetration depth of the biocide, a, at a given time is defined as the depth into the film where the concentration of the biocide falls to zero, and can be found from a matching flux equation:

$$\frac{D_e C_b}{a} = \frac{X_b}{Y_{xb}} \frac{da}{dt}.$$

The left-hand term describes the flux of antimicrobial agent through the layer of biomass in which the neutralizing capacity of the biomass has been depleted. The right-hand term describes the rate of advance of the penetration front. When integrated once, with the initial condition $z = 0$ at $t = 0$, this yields

$$\frac{a^2}{2} = \frac{D_e C_b Y_{xb}}{X_b} t.$$

This is rearranged to give two very useful equations that describe the time required to penetrate to a point within the biofilm:

$$a = \left(\frac{2D_e C_b Y_{xb}}{X_b} t\right)^{1/2} \tag{6}$$

and

$$t = \frac{a^2 X_b}{2D_e C_b Y_{xb}}. \tag{7}$$

Returning to (1) and integrating the case where $t \leq t_{pen}$, which includes the first two boundary conditions in (5), leads to

$$\ln\left(\frac{X}{X_o}\right) = -k_{dis}\int_0^{t_1} 0\, dt - kC_b\int_{t_1}^{t_{dose}} dt + k_{dis}C_b\int_{t_1}^{t_{dose}} \frac{z}{a}\, dt.$$

Solving for the penetration depth, a, by substituting Eq. (6) into the integral, and drawing the constants derived from that outside the integral:

$$\ln\left(\frac{X}{X_o}\right) = -k_{dis}C_b(t_{dose} - t_1) + k_{dis}C_b\left(\frac{X_b}{2D_e C_b Y_{xb}}\right)^{1/2} z\int_{t_1}^{t_{dose}} t^{-1/2}\, dt.$$

The final unknown time parameter, t_1, can be found with the substitution of (7):

$$\ln\left(\frac{X}{X_o}\right) = -k_{dis}C_b\left(t_{dose} - \frac{z^2 X_b}{2C_b D_e Y_{xb}}\right) + \ldots k_{dis}C_b\left(\frac{X_b}{2D_e C_b Y_{xb}}\right)^{1/2} z2\left(t_{dose}^{1/2} - \left(\frac{z^2 X_b}{2C_b D_e Y_{xb}}\right)^{1/2}\right). \tag{8}$$

To simplify this unwieldly expression, some grouping of constants proves useful:

$$\psi \equiv k_{dis}C_b t_{dose}, \quad \xi \equiv \frac{z}{L_f}, \quad \tau \equiv \frac{t_{dose}}{t_{pen}} = \frac{2D_e C_b Y_{xb} t_{dose}}{L_f^2 X_b},$$

which then transforms Eq. (8) into a nice form:

$$\ln\left(\frac{X}{X_o}\right) = -\psi + \frac{\psi}{\tau}\xi^2 + \frac{2\psi}{\sqrt{\tau}}\xi - \frac{2\psi}{\tau}\xi^2,$$

$$\ln\left(\frac{X}{X_o}\right) = -\psi(\tau^{-1}\xi^2 - 2\tau^{-1/2}\xi + 1),$$

$$\ln\left(\frac{X}{X_o}\right) = -\psi(\tau^{-1/2}\xi - 1)^2. \tag{9}$$

Integration of the system of equations with respect to the dimensionless spatial parameter, ξ, over the entire depth of the biofilm generates an average survival fraction. Several of the limits of integration include the penetration depth into the biofilm, a, which was solved for using Eq. (6) previously. Rather than expand a into the bulky form as seen before, it is advantageous to use an alternative form of τ.

$$\frac{a}{L_f} = \left(\frac{2D_e C_b Y_{xb}}{X_b L_f^2} t\right)^{1/2} = \tau^{1/2}.$$

The average survival fraction is then defined as:

$$\int_0^1 \frac{X}{X_o}\, d\xi = \int_{\tau^{1/2}}^1 \exp(0)\, d\xi + \int_0^{\tau^{1/2}} \exp(-\psi(\tau^{-1/2}\xi - 1)^2) d\xi \quad \text{for} \quad t_{dose} \leq t_{pen}. \tag{10}$$

To examine the case where $t_{dose} > t_{pen}$, Eq. (5) must be solved for all three conditions, again going through all the machinations previously described:

$$\ln\left(\frac{X}{X_o}\right) = -k_{dis}\int_0^{t_1} 0\, dt - kC_b\int_{t_1}^{t_{pen}} dt + k_{dis}C_b\int_{t_1}^{t_{pen}} \frac{z}{a}\, dt - k_{dis}C_b\int_{t_{pen}}^{t_{dose}} dt,$$

$$\ln\left(\frac{X}{X_o}\right) = -\frac{\psi}{\tau}(\xi^2 - 2\xi + \tau) \quad \text{for} \quad t_{dose} > t_{pen},$$

$$\int_0^1 \frac{X}{X_o}\, d\xi = \int_0^1 \exp\left(-\frac{\psi}{\tau}(\xi^2 - 2\xi + \tau)\right) d\xi.$$

Once the solutions are combined, the final solution is:

$$\int_0^1 \frac{X}{X_o}\, d\xi = \begin{cases} \int_{\tau^{1/2}}^1 \exp(0)\, d\xi + \int_0^{\tau^{1/2}} \exp(-\psi(\tau^{-1/2}\xi - 1)^2 d\xi & \text{for} \quad t_{dose} \leq t_{pen}, \\ \int_0^1 \exp\left(-\frac{\psi}{\tau}(\xi^2 - 2\xi + \tau)\right) d\xi & \text{for} \quad t_{dose} > t_{pen}. \end{cases} \tag{11}$$

Catalytic Transport Model

When catalytic reaction of an antimicrobial agent occurs in a biofilm, the capacity of the biofilm to degrade the agent does not diminish in time. Examples of such a situation are the disproportionation of hydrogen peroxide by catalase or the deactivation of β-lactam antibiotics by β-lactamase enzymes. In these cases a steady state balance between reaction and diffusion will be quickly established in the biofilm leading to a static concentration profile. The extent of penetration is determined by a Thiele modulus, a dimensionless parameter that characterizes the balance of reaction and diffusion process rates (Fig. 1C). Unlike the stoichiometric transport model presented above, the catalytic transport model encompasses the possibility that the antimicrobial agent will never fully penetrate the biofilm. If the Thiele modulus is greater than 1, the agent will not reach the substratum, thereby leaving a fraction of the biofilm unchallenged.

The catalytic transport model is derived by combining the basic disinfection model (1) with a concentration profile determined by a simple reaction-diffusion model. Zero-

order reaction kinetics are assumed. The governing differential equation for a steady-state diffusion and reaction when the reaction follows zero-order kinetics is

$$D_e \frac{d^2C}{dz^2} = -k_o,$$

which, through the use of the following definitions:

$$u \equiv \frac{C}{C_b}, \quad \xi \equiv \frac{z}{L_f}, \quad \phi^2 \equiv \frac{k_o L_f^2}{2D_e C_b}, \tag{12}$$

becomes

$$\frac{d^2u}{d\xi^2} = 2\phi^2. \tag{13}$$

It is unknown what kind of penetration profiles to expect. Therefore, the differential equation must be integrated with two sets of boundary conditions:

$$\begin{cases} 1)\ u = 1 \text{ at } \xi = 0 \\ 2)\ u = 0 \text{ at } \xi = \dfrac{a}{L_f} \end{cases}$$

when the biofilm is not fully penetrated, and

$$\begin{cases} 1)\ u = 1 \text{ at } \xi = 0 \\ 2)\ \dfrac{du}{d\xi} = 0 \text{ at } \xi = 1 \end{cases}$$

when the biofilm is fully penetrated. The penetration depth, a, is defined as the depth into the biofilm at which the antimicrobial agent concentration is zero.

Integrating Eq. (13) twice with respect to the spatial variable, ξ, using the boundary conditions above, produces the solutions

$$\begin{cases} u = 0, & \dfrac{a}{L_f} < \xi \le 1 \\ u = \phi^2\xi^2 - 2\phi\xi + 1, & 0 < \xi \le \dfrac{1}{L_f} \end{cases} \tag{14}$$

when the biofilm is not fully penetrated, and

$$u = \phi^2\xi^2 - 2\phi^2\xi + 1$$

when the biofilm is fully penetrated;

$$a \equiv (2D_e C_b / k_o)^{1/2}$$

Once these parameters have been found, the basic planktonic disinfection model (1) must be coupled with the predicted concentration profiles.

This can now be transformed and integrated, using the substitutions in (12) to arrive at

$$\ln\left(\frac{X}{X_o}\right) = -\psi u(\xi), \tag{15}$$

where $\psi \equiv k_{dis} t_{dose} C_b$ and

$$\ln\left(\frac{X}{X_o}\right) = \begin{cases} \begin{cases} -\psi[\phi^2\xi^2 - 2\phi\xi + 1] & \text{for} \\ \quad 0 \le \xi \le \dfrac{a}{L_f} \text{ and } \left(\dfrac{a}{L_f} < 1 \text{ or } \phi \ge 1\right), \\ 0 \quad \text{for} \quad \dfrac{a}{L_f} \le \xi \le 1 \end{cases} \\ -\psi[\phi^2\xi^2 - 2\phi^2\xi + 1] \quad \text{for} \\ \quad \left(\dfrac{a}{L_f} = 1 \text{ or } \phi < 1\right). \end{cases}$$

From this solution, integration with respect to the spatial parameter, ξ, over the entire depth of the biofilm generates an average survival fraction:

$$\int_0^1 \frac{X}{X_o} d\xi = \begin{cases} \int_{a/L_f}^1 \exp(0)\, d\xi + \int_0^{a/L_f} \exp(-\psi[\phi^2\xi^2 \\ \quad - 2\phi\xi + 1])d\xi \quad \text{for} \\ \quad \left(\dfrac{a}{L_f} < 1 \text{ or } \phi \ge 1\right), \\ \int_0^1 \exp(-\psi[\phi^2\xi^2 - 2\phi^2\xi + 1])d\xi \\ \quad \text{for} \quad \left(\dfrac{a}{L_f} = 1 \text{ or } \phi < 1\right). \end{cases} \tag{16}$$

Table I summarizes the three models, showing the degrees of freedom of each, the parameters used, and the physical significance of the model.

MATERIALS AND METHODS

Biofilm Disinfection

Alginate gel bead artificial biofilms were prepared and disinfected as described elsewhere (Xu et al., 1996; Stewart et al., 1998). *P. aeruginosa* were incorporated into 2-mm diameter gel beads which were then incubated overnight in nutrient broth to allow the microorganisms to adapt to the biofilm mode of growth. Disinfection was performed by suspending approximately 300 gel beads in 500 mL of pH 7.2 phosphate buffer containing 10 mg/L of sodium hypochlorite and 5 m*M* calcium chloride. The hypochlorite solution was periodically decanted and replenished to maintain the bulk fluid free chlorine residual at the desired concentration. Chlorine concentrations were confirmed by the DPD colorimetric method (Hach). Gel beads were removed from the disinfectant solution at regular intervals and immediately transferred to a tube containing 50 m*M* sodium thiosulfate to neutralize residual chlorine. The beads were dissolved by allowing them to stand in 50 m*M* sodium citrate buffer (pH 7.2) at 4°C for 1–2 h. The resulting cell suspension was then serially diluted and drop-plated to enumerate surviving bacteria.

Data Fitting

The mathematical software package, MATLAB, was used to implement the models (The MathWorks, 1998). Four sets

of experimental data were examined. A constrained minimization technique was used to establish the values for the parameters used in each permutation of the models. This was necessary because, as previously described, an analytical solution to the models was not generally possible. Generally, the analysis followed three steps. First, the user defined the data set, bulk fluid concentrations, and as many other parameters as possible given available information. Second, the remaining parameters were constrained, or given maximum and minimum values, and initial guesses for the parameters were made. Third, a constrained minimization routine was called to run each of the three models. Briefly, the minimization routine attempted to find the parameters values within the ranges specified that minimized the sum of the squared residual error between the actual data and the theoretical prediction based on the parameters.

When possible, independent measurements were used for as many parameters as possible. In most cases, the disinfection rate constant, bulk antimicrobial agent concentration, and dose times were the only parameters that could be independently determined. To take into account the variable number of parameters in the model the Akaike Information Criterion (AIC) was invoked to weigh the degrees of freedom (DOF) and sum of the squared residual error (RSS) generated from fitting a number of experimental data points (n) (Venables and Ripley, 1994). As the AIC, defined below, decreased, the model was deemed a better fit.

$$\mathrm{AIC} = n \ln(RSS/n) + 2\mathrm{DOF}. \qquad (17)$$

RESULTS

General Model Features

Three dynamic models of biofilm killing by antimicrobial agents, each embodying a distinct mechanism of biofilm resistance, were derived. The three models predicted different microbial survival versus time (or concentration) dependence (Fig. 2). The physiological limitation model predicted characteristic biphasic killing (Fig. 2A). Biofilm killing was proportional to the product of antimicrobial dose concentration and dose duration according to the physiological limitation model. Killing curves predicted by the physiological limitation model were always concave up. In contrast, killing curves predicted by the stoichiometric transport model were always concave down (Fig. 2B). Little killing occurred, according to this model, until the antimicrobial agent had penetrated the biofilm fully. Once the biofilm had been completely penetrated, rapid disinfection was possible. Like the physiological limitation model, the stoichiometric transport model required that biofilm killing was proportional to the product of antimicrobial dose concentration and dose duration. As did the other two models, the catalytic transport model predicted nonlinear survival curves (Fig. 2C). These curves exhibited a concave up shape. Unlike the other two models, killing predicted by the catalytic transport model was not directly proportional to the product of anti-

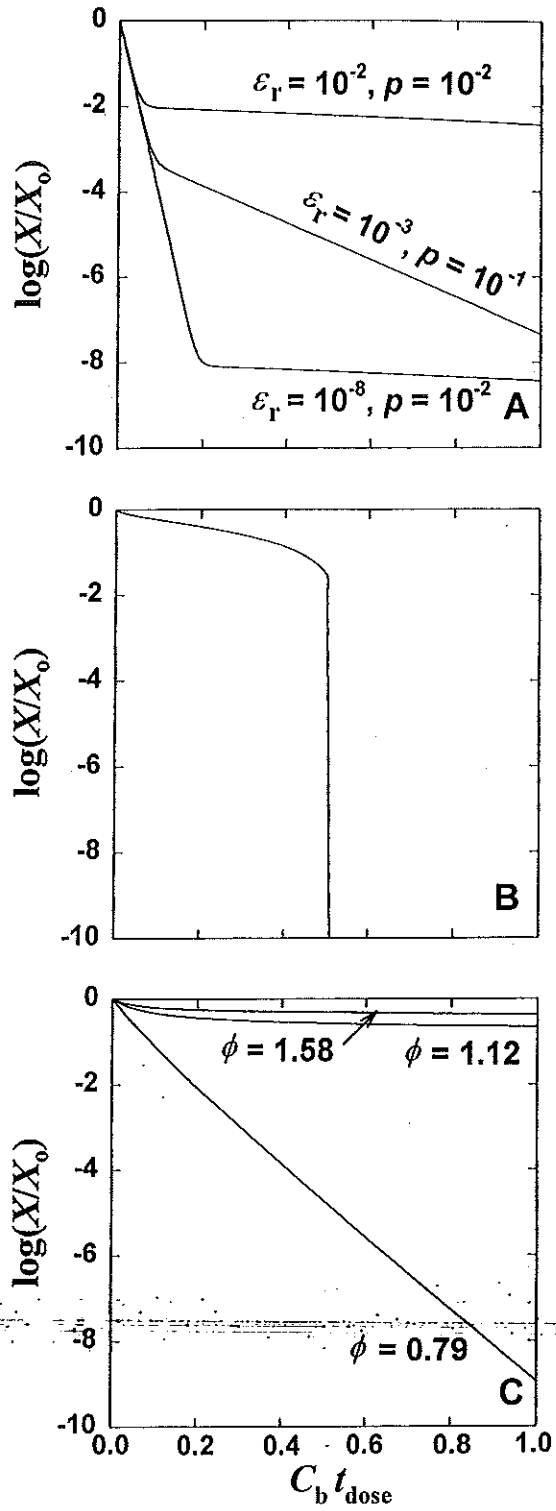

Figure 2. Predicted overall biofilm survival versus dose (antimicrobial concentration × dose duration) for three models of biofilm resistance to antimicrobial agents. The dose has arbitrary units. (A) Physiological limitation model for three cases with different resistant subpopulation fractions (ε_r) and relative susceptibilities of the resistant population (p). Biofilm survival is independent of dose concentration when plotted versus $C_b t_{dose}$. (B) Stoichiometric transport model. Biofilm survival is independent of dose concentration when plotted versus $C_b t_{dose}$. (C) Catalytic transport model. Biofilm survival changes with differing bulk antimicrobial concentrations, which are indicated by corresponding values of the Thiele modulus.

Table II. Summary of experimental data sets.

Microorganism	Biofilm age (days)	Initial cell density (cfu/cm^2)	Agent	Concentration (mg/L)	Citation
P. aeruginosa	2	3×10^7	Tobramycin	20	Anwar et al., 1998a,b
P. aeruginosa	NA	3×10^8	Hypochlorite at pH 7	10	This work
P. aeruginosa	3	6×10^9	Hydrogen peroxide	1,700	This work
P. aeruginosa	7	2×10^9	Tobramycin	200	Anwar et al., 1998a,b

microbial dose concentration and dose duration. Higher concentrations of antimicrobial agent always yielded improved disinfection, even when a proportional decrease in the dose duration was implemented (Fig. 2C).

Four sets of experimental data on biofilm killing versus time were fit to the models described above. All four of the data sets pertain to pure cultures of *Pseudomonas aeruginosa,* so while there are differences in the biofilm culture methods and antimicrobial agents, the fundamental microbiology is similar. There were two broad objectives to this data fitting analysis. The first was to determine whether any of the models could reasonably capture experimentally observed phenomena. A second objective was to gain insight into the possible resistance mechanisms that were operative in a particular case. Important features of the experimental data sets are summarized in Table II. Results of the model fitting are summarized in Table III and are discussed case by case below.

Two-Day-Old *P. aeruginosa* Biofilm Challenged with Tobramycin

Anwar and co-workers (1989a,b) grew iron-limited biofilms of *P. aeruginosa* in a chemostat and challenged these biofilms with the aminoglycoside antibiotic, tobramycin. The first data set, shown in Figure 3, is a disinfection time series over 5 hours on a 2-day-old biofilm. The physiological limitation model fit the data best according to the AIC measure. The fitted parameter values indicated that the resistant subpopulation within the biofilm constituted only 2.6% of the total cell population. This resistant population exhibited a disinfection rate coefficient that was 2 orders of magnitude smaller than that measured for planktonic cells. The catalytic transport model fit the data less well, though it did capture approximately the right shape. The stoichiometric transport model was not able to fit this data set adequately as it is incapable of predicting a concave up curve shape.

Table III. Ranking of model fits by the AIC measure for each experimental data set.[a]

Rank	2-Day-old biofilm, tobramycin	Gel bead biofilm, hypochlorite	3-Day-old biofilm, hydrogen peroxide	7-Day-old biofilm, tobramycin
1	**P**	**S**	**P**	**C**
2	C	C	C	P
3	S	P	S	S

[a]The model selected after consideration of other factors is in boldface. Model designations are as defined in Table I.

Artificial *P. aeruginosa* Biofilm Challenged with Hypochlorous Acid

P. aeruginosa cells entrapped in alginate gel bead artificial biofilms were challenged with 10 mg/L chlorine at neutral pH. The shape of the disinfection curve in this case clearly implies a stoichiometric transport limitation (Fig. 4). The physiological limitation and catalytic transport models fit this data set very poorly as both of those models are incapable of predicting a concave down curve. The time required to fully penetrate the biofilm, according to the stoichiometric transport model fit, was approximately 97 min.

P. aeruginosa Biofilm Challenged with Hydrogen Peroxide

P. aeruginosa biofilms challenged for 1 h with 50 m*M* hydrogen peroxide resisted killing (Fig. 5) (Elkins et al.,

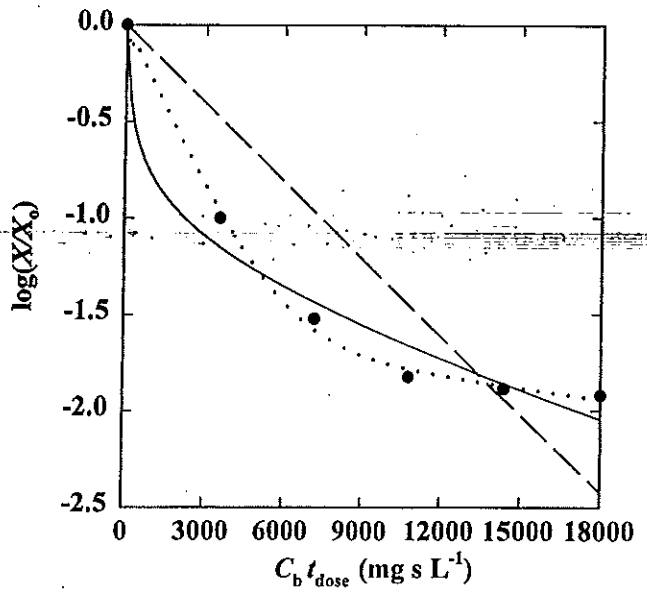

Figure 3. Survival of 2-day-old *P. aeruginosa* biofilms treated with tobramycin with fits for the physiological limitation model (dotted line), stoichiometric transport model (dashed line), and catalytic transport model (solid line).

Marrie TJ. 1987. Bacterial biofilms in nature and disease. Annu Rev Microbiol 41:435–464.

Costerton JW, Stewart PS, Greenberg EP. 1999. Bacterial biofilms: A common cause of persistent infections. Science 284:1318–1322.

Darouiche RO, Dhir A, Miller AJ, Landon GC, Raad II, Musher DM. 1994. Vancomycin penetration into biofilm covering infected prostheses and effect on bacteria. J Infect Dis 170:720–723.

de Beer D, Srinivasan R, Stewart PS. 1994. Direct measurement of chlorine penetration into biofilms during disinfection. Appl Environ Microbiol 60:4339–4344.

Desai M, Weller PH, Brown MRW. 1998. Increasing resistance of planktonic and biofilm cultures of *Burkholderia cepacia* to ciprofloxacin and ceftazidime during exponential growth. J Antimicrob Chemother 42:153–160.

Dibdin GH, Assinder SJ, Nichols WW, Lambert PA. 1996. Mathematical model of β-lactam penetration into a biofilm of *Pseudomonas aeruginosa* while undergoing simultaneous inactivation by released β-lactamases. J Antimicrob Chemother 38:757–769.

Dunne WM Jr, Mason EO Jr, Kaplan SL. 1993. Diffusion of rifampin and vancomycin through a *Staphylococcus epidermidis* biofilm. Antimicrob Agents Chemother 37:2522–2526.

Elkins JG, Hassett DJ, Stewart PS, Schweizer HP, McDermott TR. 1999. *Pseudomonas aeruginosa* biofilm resistance to hydrogen peroxide: Protective role of catalase. Appl Environ Microbiol 65:4594–4600.

Foley I, Marsh P, Wellington EMH, Smith AW, Brown MRW. 1999. General stress response master regulator rpoS is expressed in human infection: A possible role in chronicity. J Antimicrob Chemother 43: 164–165.

Gilbert P, Brown MRW. 1995. Mechanisms of the protection of bacterial biofilms from antimicrobial agents. In: Lappin-Scott HM, Costerton JW, editors. Microbial Biofilms. Cambridge: Cambridge University Press. p 118–130.

Hassett DJ, Elkins JG, Ma J-F, McDermott TR. 1999. *Pseudomonas aeruginosa* biofilm sensitivity to biocides: Use of hydrogen peroxide as a model antimicrobial agent for examining resistance mechanisms. Methods Enzymol 310:599–608.

Huang C-T, Xu KD, McFeters GA, Stewart PS. 1998. Spatial patterns of alkaline phosphatase expression within bacterial colonies and biofilms in response to phosphate starvation. Appl Environ Microbiol 64: 1526–1531.

Liu X, Roe F, Jesaitis A, Lewandowski Z. 1998. Resistance of biofilms to the catalase inhibitor 3-amino-1,2,4-triazole. Biotechnol Bioeng 59: 156–162.

The MathWorks, Inc. 1998. MATLAB, Version 5.2.0.3084. Watick, MA.

Nichols WW, Evans MJ, Slack MPE, Walmsley HL. 1989. The penetration of antibiotics into aggregates of mucoid and non-mucoid *Pseudomonas aeruginosa*. J Gen Microbiol 135:1291–1303.

Shigeta M, Tanaka G, Komatsuzawa H, Sugai M, Suginaka H, Usui T. 1997. Permeation of antimicrobial agents through *Pseudomonas aeruginosa* biofilms: A simple method. Chemotherapy 43:340–345.

Siegrist H, Gujer W. 1987. Demonstration of mass transfer and pH effects in a nitrifying biofilm. Wat Res 21:1481–1487.

Stewart PS. 1994. Biofilm accumulation model that predicts antibiotic resistance of *Pseudomonas aeruginosa* biofilms. Antimicrob Agents Chemother 38:1052–1058.

Stewart PS. 1996. Theoretical aspects of antibiotic diffusion into microbial biofilms. Antimicrob Agents Chemother 40:2517–2522.

Stewart PS. 1998. A review of experimental measurements of effective diffusive permeabilities and effective diffusion coefficients in biofilms. Biotechnol Bioeng 59:261–272.

Stewart PS, Grab L, Diemer JA. 1998. Analysis of biocide transport limitation in an artificial biofilm system. J Appl Microbiol 85:495–500.

Stewart PS, Hamilton MA, Goldstein BR, Schneider BT. 1996. Modeling biocide action against biofilms. Biotechnol Bioeng 49:445–455.

Stewart PS, Raquepas JB. 1995. Implications of reaction-diffusion theory for the disinfection of microbial biofilms by reactive antimicrobial agents. Chem Eng Sci 50:3099–3104.

Suci P, Mittelman MW, Yu FP, Geesey GG. 1994. Investigation of ciprofloxacin penetration into *Pseudomonas aeruginosa* biofilms. Antimicrob Agents Chemother 38:2125–2133.

van Stroe-Biezen SAM, Everaerts FM, Janssen LJJ, Tacken RA. 1993. Diffusion coefficients of oxygen, hydrogen peroxide, and glucose in a hydrogel. Anal Chim Acta 273:553–560.

Venables WN, Ripley BD. 1994. Modern Applied Statistics with S-Plus. New York: Springer-Verlag.

Vrany JD, Stewart PS, Suci PA. 1997. Comparison of recalcitrance to ciprofloxacin and levofloxacin exhibited by *Pseudomonas aeruginosa* biofilms displaying rapid-transport characteristics. Antimicrob Agents Chemother 41:1352–1358.

Wentland E, Stewart PS, Huang C-T, McFeters GA. 1996. Spatial variations in growth rate within *Klebsiella pneumoniae* colonies and biofilm. Biotechnol Prog 12:316–321.

Xu KD, Stewart PS, Xia F, Huang C-T, McFeters GA. 1998. Spatial physiological heterogeneity in *Pseudomonas aeruginosa* biofilm is determined by oxygen availability. Appl Environ Microbiol 64: 4035–4039.

Xu X, Stewart PS, Chen X. 1996. Transport limitation of chlorine disinfection of *Pseudomonas aeruginosa* entrapped in alginate beads. Biotechnol Bioeng 49:93–100.